

Directional Etching of Silicon by Silver Nanostructures

Pradeep Sharma^{1,2,3} and Yuh-Lin Wang^{1,2,3*}

¹Institute of Atomic and Molecular Sciences, Academia Sinica, Taipei, Taiwan 10617, R.O.C.

²Department of Physics, National Taiwan University, Taipei, Taiwan 10617, R.O.C.

³Nano Science and Technology Program, Taiwan International Graduate Program, Academia Sinica, Taipei, Taiwan 11529, R.O.C.

Received November 5, 2010; accepted December 20, 2010; published online January 18, 2011

We report directional etching of nanostructures (nanochannels and nanotrenches) into the Si(100) substrates in aqueous HF and H₂O₂ solution by lithographically defined Ag patterns (nanoparticles, nanorods, and nanorings). The Effect of Ag/Si interface oxide on the directional etching has been studied by etching Ag/SiO_x/Si samples of known interface oxide thickness. Based on high resolution transmission electron microscopy (HRTEM) imaging and TEM-energy dispersive X-ray (EDX) spectra of the Ag/Si interfaces, we propose that maintenance of the sub-nanometer oxide at the Ag/Si interfaces and Ag–Si interaction are the key factors which regulate the directional etching of Si.

© 2011 The Japan Society of Applied Physics

Metal assisted chemical etching (MACE) of Si is defined as etching of Si in an aqueous solution of HF and metal salts.¹⁾ It can also be conducted in an aqueous solution of HF and an oxidizing agent, such as H₂O₂, after deposition of noble metal thin films or nanoparticles (NPs) or lithographic patterns onto Si. MACE has been conducted to improve the photoluminescence of Si,²⁾ enhance the photovoltaic efficiency of solar cells,³⁾ site selective etching of Si,⁴⁾ fabricate Si nanostructures,^{1,5,6)} create super-hydrophobic surfaces,⁷⁾ and to etch three dimensional nanostructures into Si by lithographically defined Au patterns.⁸⁾

Directional etching of Si(100) substrates by Ag nanoparticles and Ag meshes has been reported by different groups.^{1,5,6)} However, directional etching of Si by isolated Ag nanorods and nanorings has not been achieved. Furthermore, it has been observed that etching proceeds by reduction of H₂O₂ on a Ag surface accompanied by oxidation of Si and followed by etching of the oxidized Si by HF.^{1,6)} The etching of formed silicon oxide by HF is isotropic, which implies that Ag/Si interface oxide is a key factor which governs the directionality of Si etching. However, the role of interface oxide remains unknown.

In this work, we perform the directional etching of the Si(100) substrates by Ag nanoparticles, Ag nanorods, and Ag nanorings. After the etching of a Ag/Si sample, the oxide at Ag/Si interface is examined using high resolution transmission electron microscopy (HRTEM). The Effect of Ag/Si interface oxide on the directional etching is studied by etching of Ag/SiO_x/Si samples of known interface oxide thickness. A mechanism based on Ag–Si interaction has been proposed to explain the directional etching of Si by Ag.

To perform the directional etching of a Si(100) substrate by lithographically defined Ag nanoparticles, nanorods, and nanorings, Ag nanopatterns are fabricated on the Si substrates using scanning electron microscopy (SEM)-based electron beam lithography (EBL). First, poly(methyl methacrylate) (PMMA) A4 is spin coated on a clean and dry H–Si substrate to achieve a PMMA thickness of 200 nm. After baking the coated Si substrate at 180 °C for 3 min, it is loaded into the SEM-based EBL system for writing the desired patterns onto PMMA. Then, an electron beam patterned PMMA/Si sample is developed in the 3 : 1 (v/v) solution of methyl isobutyl ketone (MIBK) and iso propyl

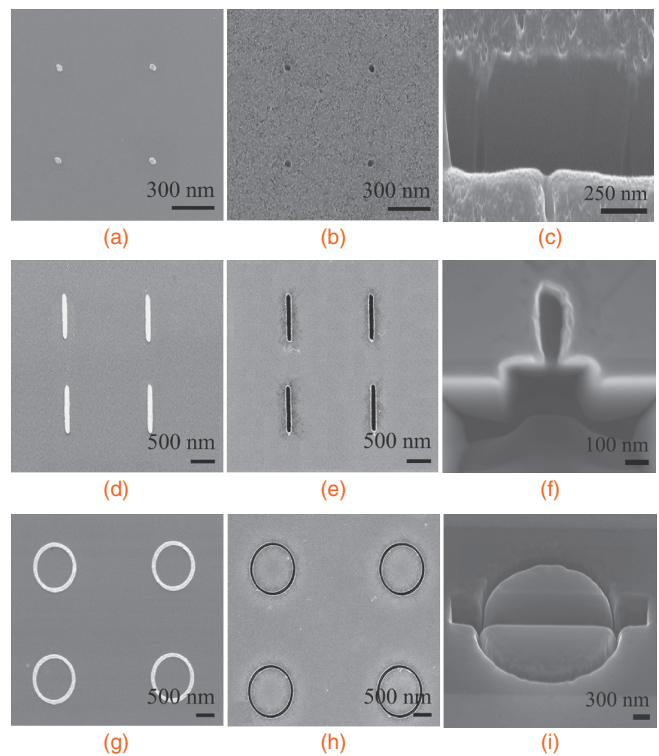


Fig. 1. SEM images of Ag nanopatterns on Si: (a) Ag nanoparticles, (d) Ag nanorods, and (g) Ag nanorings. SEM images of the corresponding etched Si nanostructures formed after etching Ag nanopattern/Si in aqueous solutions of 4.8 M HF and 0.3 M H₂O₂ for 10 min: (b)–(c), (e)–(f), and (h)–(i).

alcohol (IPA) for 1 min, followed by rinsing in IPA for 30 s, rinsing in de-ionized water for 5 s, and blow drying using dry nitrogen gas. Any residual PMMA and Si native oxide on the sample are removed by 5 s carbon–tetra fluoride (CF₄) reactive ion etching (RIE) at 50 W power and 20 mTorr pressure. Then, the cleaned sample is immediately loaded into an oil-free thermal evaporator for deposition of a 50 nm Ag thin film. Afterwards, a lift-off process is conducted in Remover PG (Micro-Chem) to obtain the desired Ag nanopatterns on Si, followed by the etching in the aqueous solution of 4.8 M HF and 0.3 M H₂O₂. SEM characterization is performed to record the morphologies of all the Ag nanopatterns on Si and the etched Si substrates. Figures 1(a), 1(d), and 1(g) show the SEM images of the Ag nanoparticles, nanorods, and nanorings on the Si substrate

*E-mail address: ylwang@pub.iams.sinica.edu.tw

respectively, whereas Figs. 1(b), 1(e), and 1(h) show the plan view SEM images of the corresponding etched nanostructures. Respective cross-sectional SEM images of the etched nanostructures in Figs. 1(c), 1(f), and 1(i) elucidate the etching of straight nanostructures into Si along [100] direction. Cross-sections of the etched nanostructures are cut using 1 pA Ga⁺ Focused Ion Beam (FIB) operating at 30 KV. We observe partial closure/covering of the etched nanostructures by the ion beam sputtered Si. It implies that top most Si surface and vicinity of the etched nanostructures have micro-porous Si structure as suggested by Chourou *et al.*¹²⁾

To understand the directional etching of Si, the Ag/Si interface is examined by HRTEM after the etching of Ag (5 nm thickness)/Si substrates in the aqueous solution of 4.8 M HF and 0.3 M H₂O₂. The Ag (5 nm thickness)/Si sample is chosen for ease of characterization. Ag film deposition is conducted by radio frequency magnetron sputtering of a Ag target (99.99% purity) under an Ar gas pressure of 2 mTorr. In order to record the Ag/Si interface with a minimal effect from air oxidation, the etched Si substrates are dried up quickly and covered with commercial G1 glue. Thereafter, the G1 glue is cured at 180 °C for 3 min to cross link the epoxy to terminate the Si oxidation process.⁹⁾ It is known that the Si oxidation rate ($\approx 2\text{--}5 \text{ \AA}$ in about 5 h) is very low,¹⁰⁾ at standard temperature and pressure (S.T.P.) and quick coverage with the G1 glue also terminates this process. Cross-sectional HRTEM samples are prepared quickly to limit the oxidation of Si during the sample preparation followed by loading of samples into the microscope. TEM-energy dispersive X-ray (EDX) spectra are used to quantify the amount of SiO_x present at the Ag/Si interface after the etching of Si by Ag. Etching of the Ag/Si sample results in the formation of straight nanochannels along the Si [100] direction as shown in Fig. 2(a). Figure 2(b) shows the cross-sectional TEM image of a Ag NP at the bottom of a Si nanochannel. Here, the region marked “1” is the location of a thinner Ag/Si interface oxide and that marked “2” is the location of a thicker Ag/Si interface oxide. Figure 2(c) shows the cross-sectional HRTEM image of the very thin SiO_x at the Ag/Si interface (within the regions enclosed by white circles). TEM-EDX spectra from the regions marked “1” and “2” in Fig. 2(b) are shown in Fig. 2(d) which reveals that the silicon to oxygen ratio is about 3–4 times higher in the region marked “1”. We conducted investigation of 10 Ag NPs which are randomly selected from different etched Si samples and all Ag NPs show similar type of etching interfaces. These results imply that at any given time, two types of locations are present during the etching process. At type-a locations [e.g., the region marked “1” in Fig. 2(b)], Ag NPs remain in contact with Si, whereas at type-b locations [e.g., the region marked “2” in Fig. 2(b)], oxidation of Si and etching of the formed oxide continue. TEM sample preparation may result in formation of additional SiO_x at Ag/Si interface. Therefore, we are considering only relative amount of SiO_x at different types of Ag/Si interfaces. Maintenance of the Ag–Si nano-scale contacts or very thin SiO_x mediated Ag–Si interaction results in the charge neutrality of Ag NPs which in turn ensures that Ag NPs are not etched during the etching process. Otherwise, if Ag NPs are not in contact with Si or

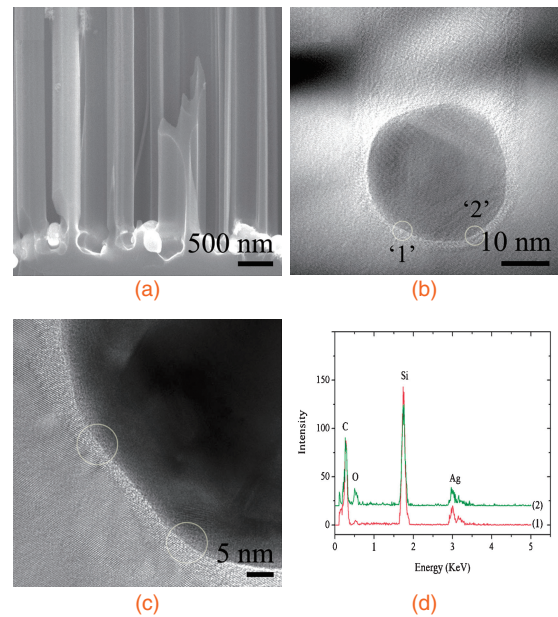


Fig. 2. Cross-sectional SEM image of Si nanochannels formed after etching of Ag (5 nm film)/Si in aqueous solutions of 4.8 M HF and 0.3 M H₂O₂ for 10 min. (b) HRTEM image of a single Ag nanoparticle at bottom of etched Si nanochannel. (c) Zoom-in HRTEM image showing a thin nano-scale Ag/Si interface within the regions enclosed by white circles. (d) TEM-EDX spectra recorded from locations marked “1” and “2” in image (b).

Ag–Si interaction is too weak, Ag NPs will be oxidized by H₂O₂ and etched away by HF.

Our results suggest that SiO_x is an intermediate in Ag assisted Si etching. Therefore, to understand the effect of Ag/Si interface oxide on the directional etching of Si, the Ag thin film deposited Si samples with various Ag/Si interface oxide thicknesses are etched in the aqueous solution of 4.8 M HF and 0.3 M H₂O₂. First, clean hydrogen terminated Si substrates are prepared. Then, on one substrate, the Ag thin film (thickness $\approx 5 \text{ nm}$) is sputter deposited. Immediately after deposition, it is etched in the etching solution. Other cleaned Si substrates are oxidized in a humid-pure oxygen environment to achieve 5–7- and 10–12- \AA -thick silicon oxides.¹⁰⁾ After depositing Ag, the samples are immediately etched in the etching solution. After etching of Ag/SiO_x (2–3 \AA)/Si and Ag/SiO_x (5–7 \AA)/Si samples, the formation of directional nanochannels by the Ag nanoparticles into Si is observed [Figs. 3(a)–3(d)], whereas etching of Ag/SiO_x (10–12 \AA)/Si results in the formation of micro-porous Si on top accompanied by reduction in the number density of straight channels as shown in Figs. 3(e) and 3(f). Supplementary information on Fig. 3 shows that sputter deposition of Ag on SiO_x (2–3 \AA)/Si, SiO_x (5–7 \AA)/Si, and SiO_x (10–12 \AA)/Si substrates results in deposition of the Ag film with similar type of morphologies which implies that etching behavior of these Si samples is not associated with Ag film morphologies. Therefore, when the interface oxide thickness is about 1 nm, Ag nanoparticles trace random trajectories in the beginning of the etching process. Once the Ag/Si interface acquires equilibrium interface oxide thickness ($\approx 5 \text{ \AA}$), they start to perform the directional etching of nanochannels into Si. Results in Figs. 3(e) and 3(f) may also be explained by etching of many Ag NPs into

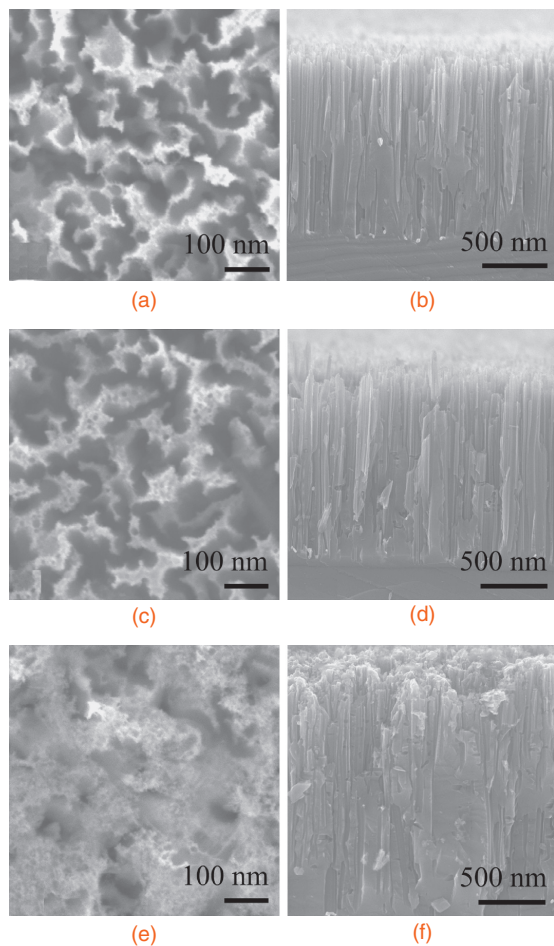
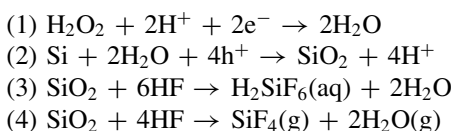


Fig. 3. SEM images of etched Si after etching of Ag/SiO_x (2–3 Å)/Si (a, b), Ag/SiO_x (5–7 Å)/Si (c, d), and Ag/SiO_x (10–12 Å)/Si (e, f) substrates in aqueous solution of 4.8M HF and 0.3M H₂O₂.

solution because of negligible Ag–Si interaction and subsequent reduction in number density of nanochannels. We propose that in addition to the crystallinity and doping of the Si substrate,¹¹ type of metal catalyst (Ag, Pt, or Pd),¹² the shape of the metal pattern on Si and the composition of the etching solution,^{13,14} the maintenance of the sub-nanometer oxide at the Ag/Si interface is also a key factor in regulating the directional etching of Si.

It has been proposed that Ag assisted etching of Si proceeds by reduction of H₂O₂ (reaction 1) on a Ag NP surface and oxidation of Si (reaction 2) due to injected holes, followed by etching of the oxidized Si (reactions 3 and 4) by HF into H₂SiF₆ and SiF₄.^{1,6} The following chemical reactions describe the etching process briefly.



Etching of the silicon oxide by HF is isotropic, which implies that reduction of H₂O₂ accompanied by oxidation of Si is the key factor which governs the directionality of Si etching. During the Ag assisted etching of Si in the aqueous HF + H₂O₂ solution, the surface of Si is mainly passivated either by –H bonds or by –OH or by –F bonds. Moreover, it is known that the charge transfer probability across the Si–

OH bond is higher than that across the Si–H or Si–F bond.¹⁵ Furthermore, the H–Si(100) or F–Si(100) surface is easy to oxidize in an aqueous or oxygen environment compared with Si(111) surface because it has a 4–5 times higher density of surface states.¹⁶ Therefore, the injection of holes along Si [100] is favored which in turn promotes directional oxidation (refer to reaction 2) and etching of Si. This proposal is consistent with the HRTEM investigation of the Ag/Si interface after the etching. The HRTEM image shows that during etching some part of the Ag NPs is always in contact with Si. This Ag–Si contact or interaction promotes directional oxidation followed by etching by HF. This Ag–Si interaction may also explain the sticking of Ag to Si during etching. Wei *et al.*¹⁷ calculated the adsorption energy of the Ag adatoms at a distance of one monolayer from the Si surface and found it to be about 2.4 eV. This adsorption energy would translate into an interaction force of about 10^{–9} N between the Ag adatom and the Si surface. During etching, if 1000 atoms of Ag are in contact with Si, the Ag–Si interaction force (≈10^{–7} N) is sufficient for countering Brownian force ($F_B \approx K_B T / \text{size of the Ag nanopattern}$, where K_B is the Boltzman constant; $F_B \approx 10^{-14}$ N for 50 nm Ag nanoparticles), and the force generated by bursting of gas bubbles (pressure inside the nanometer air bubble ≈ 10 MPa which is equivalent to force of 10^{–8} N). Nonetheless, if the Ag–Si interaction is weakened by excess interface oxide, the loss of directionality of etching will be observed as shown in Fig. 3.

In conclusion, directional etching of the nanostructures into Si by different Ag nanopatterns has been achieved. We propose that the sticking of Ag to Si during etching and directional etching by Ag depend on Ag/Si interface oxide thickness.

Acknowledgment One of the authors, Pradeep Sharma, wishes to acknowledge the financial support from the Taiwan International Graduate Program of Academia Sinica, Taiwan.

- 1) K. Peng, A. Lu, R. Zhang, and S.-T. Lee: *Adv. Funct. Mater.* **18** (2008) 3026.
- 2) X. Li and P. W. Bohn: *Appl. Phys. Lett.* **77** (2000) 2752.
- 3) D. H. Wan, H. L. Chen, S. Y. Chuang, C. C. Yu, and Y. C. Lee: *J. Phys. Chem. C* **112** (2008) 20567.
- 4) S. Bauer, J. G. Brunner, H. Jha, Y. Yasukawa, H. Asoh, S. Ono, H. Böhm, J. P. Spatz, and P. Schmuki: *Electrochem. Commun.* **12** (2010) 565.
- 5) H. Zhipeng, Z. Xuanxiong, R. Manfred, L. Lifeng, L. Woo, S. Tomohiro, S. Stephan, and G. Ulrich: *Nano Lett.* **8** (2008) 3046.
- 6) C. Chartier, S. Bastide, and C. Levy-Clement: *Electrochim. Acta* **53** (2008) 5509.
- 7) Y. Xiu, L. Zhu, D. W. Hess, and C. P. Wong: *Nano Lett.* **7** (2007) 3388.
- 8) O. J. Hildreth, W. Lin, and C. P. Wong: *ACS Nano* **3** (2009) 4033.
- 9) A. Gerlach, W. Keller, J. Schulz, and K. Schumacher: *Microsyst. Technol.* **7** (2001) 17.
- 10) M. Morita, T. Ohmi, E. Hasegawa, M. Kawakami, and K. Suma: *Appl. Phys. Lett.* **55** (1989) 562.
- 11) M. L. Zhang, K. Q. Peng, X. Fan, J. S. Jie, R. Q. Zhang, S. T. Lee, and N. B. Wong: *J. Phys. Chem. C* **112** (2008) 4444.
- 12) M. L. Chourou, K. Fukami, T. Sakka, S. Virtanen, and Y. H. Ogata: *Electrochim. Acta* **55** (2010) 903.
- 13) O. J. Hildreth, W. Lin, and C. P. Wong: *ACS Nano* **3** (2009) 4033.
- 14) K. Tsujino and M. Matsumura: *Electrochim. Acta* **53** (2007) 28.
- 15) X. G. Zhang: *Electrochemistry of Silicon and Its Oxide* (Springer, New York, 2001) 1st ed., p. 122.
- 16) H. Angermann, W. Henrion, A. Roseler, and M. Rebien: *Mater. Sci. B* **73** (2000) 178.
- 17) S. Wei, W. Li, F. Zhang, and X. Zhao: *Physica B* **390** (2007) 191.